Physics Letters B 685 (2010) 253–257

Contents lists available at ScienceDirect

Physics Letters B

www.elsevier.com/locate/physletb

Structure of ^{33}Mg sheds new light on the $N = 20$ island of inversion

R. Kanungo [a,*], C. Nociforo [b], A. Prochazka [b,c], Y. Utsuno [d], T. Aumann [b], D. Boutin [c], D. Cortina-Gil [e], B. Davids [f], M. Diakaki [g], F. Farinon [b,c], H. Geissel [b], R. Gernhäuser [h], J. Gerl [b], R. Janik [i], B. Jonson [j], B. Kindler [b], R. Knöbel [b,c], R. Krücken [h], M. Lantz [j], H. Lenske [c], Y. Litvinov [b,k], K. Mahata [b], P. Maierbeck [h], A. Musumarra [l,m], T. Nilsson [j], T. Otsuka [n], C. Perro [a], C. Scheidenberger [b], B. Sitar [i], P. Strmen [i], B. Sun [b], I. Szarka [i], I. Tanihata [o], H. Weick [b], M. Winkler [b]

[a] *Astronomy and Physics Department, Saint Mary's University, Halifax, NS B3H 3C3, Canada*
[b] *GSI Helmholtzzentrum für Schwerionenforschung, D-64291 Darmstadt, Germany*
[c] *Physics Department, Justus-Liebig University, 35392 Giessen, Germany*
[d] *Japan Atomic Energy Agency, Tokai, Ibaraki 319-1195, Japan*
[e] *Universidad de Santiago de Compostela, E-15706 Santiago de Compostela, Spain*
[f] *TRIUMF, Vancouver, BC V6T 2A3, Canada*
[g] *National Technical University, Athens, Greece*
[h] *Physik Department E12, Technische Universität München, D-85748 Garching, Germany*
[i] *Faculty of Mathematics and Physics, Comenius University, 84215 Bratislava, Slovakia*
[j] *Fundamental Physics, Chalmers University of Technology, SE 412-916 Göteborg, Sweden*
[k] *Max-Planck-Institut für Kernphysik, Saupfercheckweg 1, D-69117 Heidelberg, Germany*
[l] *Universita' di Catania, 95153 Catania, Italy*
[m] *INFN-Laboratori Nazionali del Sud, 95123 Catania, Italy*
[n] *Center for Nuclear Study, University of Tokyo, Wako Shi, Saitama 351-0198, Japan*
[o] *RCNP, Osaka University, Mihogaoka, Ibaraki, Osaka 567 0047, Japan*

ARTICLE INFO

Article history:
Received 6 August 2009
Received in revised form 29 January 2010
Accepted 3 February 2010
Available online 9 February 2010
Editor: V. Metag

Keywords:
Nucleon removal or knockout reactions
Shell structure
Magic number
Radioactive beams
Eikonal model

ABSTRACT

The first reaction spectroscopy on the ground state structure of ^{33}Mg through the measurement of the longitudinal momentum distribution from the one-neutron removal reaction using a C target at 898A MeV is reported. The experiment was performed at the FRS, GSI. The distribution has a relatively narrow width (150 ± 3 MeV/c (FWHM)) and the one-neutron removal cross-section is 74 ± 4 mb. An increased contribution from the $2p_{3/2}$ orbital is required to explain the observation showing its lowering compared to existing model predictions. This provides new information regarding the configuration of ^{33}Mg and the island of inversion.

Exploring the changes in shell structure of neutron-rich nuclei has been one of the major foci of nuclear physics in recent times. The so-called island of inversion [1] around neutron-rich $N = 20$ nuclei continues to be a region of great interest. The increased separation energy of the neutron-rich Na isotopes was the first signature for the breakdown of the conventional $N = 20$ shell gap [2]. The observations of a low-lying first 2^+ excited state in ^{32}Mg [3–5] indicated the presence of deformation. The lowering of the first 2^+ excited state is found to continue progressively for ^{34}Mg [6] and ^{36}Mg [7]. Large BE(2) values were also observed for lighter $N = 20$ isotones ^{31}Na [8] and ^{30}Ne [9]. The low-lying (2^+) excited state of ^{32}Ne [10] was a signature of extension of the island of inversion to $N = 22$ for the Ne isotopes.

The cause for the quenching of the $N = 20$ shell gap has been theoretically studied in the shell model framework [11,12,14,13] where fp shell contributions are taken into account. It has been discussed that in this region due to the reduced strength of the $T = 0$ attractive monopole interaction, the $1d_{3/2}$ and $1f_{7/2}$ orbitals come closer to each other leading to deformation through np–nh neutron excitations [12,13]. The deformation increases the binding of the neutron-rich $N = 20$ isotones.

* Corresponding author.
E-mail address: ritu@triumf.ca (R. Kanungo).

0370-2693
doi:10.1016/j.physletb.2010.02.008

For a complete understanding on the evolution of the island of inversion it is crucial to understand how the nuclear orbitals across the broken $N = 20$ gap are arranged. We report here the first investigation of the structure of ^{33}Mg through the longitudinal momentum distribution from one-neutron removal from ^{33}Mg. The shape of the distribution is much narrower than predictions from the shell model with the SDPF-M interaction, suggesting a larger occupancy of neutrons in the $2p_{3/2}$ orbital. This signals a lowering of the $2p_{3/2}$ orbital. The increased p-wave occupancy has not been discussed in the recent works that debate the ground state spin of ^{33}Mg [15–17]. The present finding therefore opens a new dimension in our attempt to understand the island of inversion. A recent calculation using a Wood–Saxon potential for neutron-rich Mg isotopes discusses the near-degeneracy of the $1f_{7/2}$ and $2p_{3/2}$ orbitals in a spherical potential to be a basic element in producing deformation [18].

In-beam and beta-delayed gamma spectroscopy experiments have tried to assess the boundary of the island of inversion. Among the excited states observed for $^{25-29}$Ne, those for ^{28}Ne have been interpreted to show intruder signatures, while $^{25-27}$Ne were in agreement with normal *sd*-shell predictions [19]. On the other hand proton inelastic scattering has identified low-lying intruder states in ^{27}Ne [20] that are in agreement with a study of the ^{26}Ne(d,p) reaction [21]. The level scheme of ^{29,30}Na constructed on the basis of the beta decay of ^{29,30}Ne reflected the dominance of intruder configurations in the low-lying states [22,23]. These experiments therefore, provide signatures of intruder configurations in the excited states around $N = 20$.

It is worthwhile to point out here that the island of inversion refers to intruder orbitals in the ground states of nuclei [1,11,13]. Intruder configurations were reported for the ground state of ^{28}Ne [26]. The $3/2^-$ intruder 'core' state was found to have a spectroscopic factor (SF) of 0.32(4), in fair agreement with SDPF-M shell model predictions. The momentum distribution for this intruder component was explained by a combination of $l = 0$ and 1 contributions. A measurement of the neutron knockout from ^{32}Mg found that the ground state consists dominantly of 2p–2h $N = 20$ cross-shell configurations [27]. The SF's for the intruder $2p_{3/2}$ and the $1f_{7/2}$ orbitals were found to be 0.59(11) and 1.19(36) respectively. The abnormal spin of $1/2^+$ observed for ^{31}Mg showed a deformed ground state with an intruder configuration [28].

On the neutron-rich side of the $N = 20$ gap, the beta decay of ^{33}Mg suggested an abnormal spin of $3/2^+$ due to a 1p–1h configuration resulting from an inversion of the $d_{3/2}$ and $f_{7/2}$ orbitals [15]. The intermediate energy Coulomb excitation of ^{33}Mg populated a state at 485 keV that was attributed to a rotational excitation and suggested a $5/2^+$ spin for this state [29]. Such an excitation would support ^{33}Mg having similar deformation as observed for other nuclei in the island of inversion. The measurement of a negative magnetic moment for the ^{33}Mg ground state has however suggested a spin of $3/2^-$ with a 2p–2h configuration [16]. In this configuration, it was noted that there are an odd number of neutrons in the fp shell. Very recently the large branching ratio observed for the beta decay of ^{33}Mg to the $5/2^+$ ground state of ^{33}Al suggests the ^{33}Mg ground state to be $3/2^+$ [17]. It was proposed to have an admixture of 1p–1h with two neutrons in the $f_{7/2}$ orbital and 3p–3h with four neutrons in the $f_{7/2}$ orbital configurations for ^{33}Mg. In the proposed configurations (Fig. 4 [17]) the odd neutron occupies the $d_{3/2}$ orbital and no occupancy in the $2p_{3/2}$ orbital is discussed. In this work the ground state configuration of ^{33}Mg is investigated by measuring the momentum distribution after removal of one neutron.

The experiment was performed at the fragment separator, FRS, at GSI, Darmstadt, Germany. The schematic view of the experiment is shown in Fig. 1 where the first three foci F1–F3 of the FRS are dispersive while the last F4 is achromatic. The ^{33}Mg secondary beam was produced via the fragmentation of a 1A GeV ^{48}Ca primary beam on a 6.347 g/cm^2 thick Be target. The nuclei produced were then separated and identified by transporting them to the second dispersive focus of the FRS. Detectors placed at F1 and before the target at F2 served to identify the secondary beam on target. The plastic scintillators at F1 and F2 measure the time-of-flight (TOF) between these locations. The position on the reaction target was determined by tracking using the time projection chambers (TPC) at F2. The momentum of the incident particles can be determined from the position and the central magnetic rigidity of the first half of the FRS. In addition, it can be derived from the TOF measurement. The energy-loss (ΔE) measured using the multi-sampling ionization chamber (MUSIC) provided the charge (Z) of the nuclei. The combined information from Bρ–ΔE-TOF allowed a complete event-by-event identification of the ^{33}Mg secondary beam with less than 1% contamination.

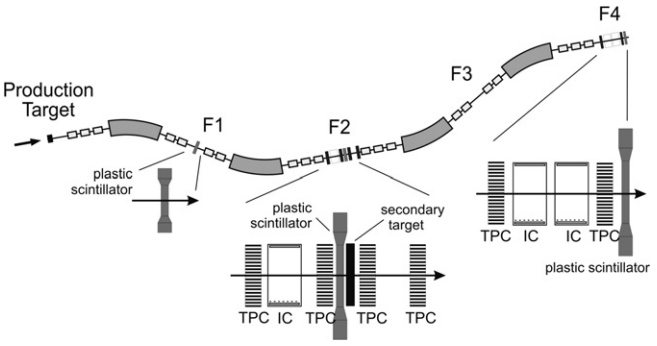

Fig. 1. Schematic setup of the experiment for one-neutron removal from ^{33}Mg using a carbon reaction target at the central focal plane of the FRS.

A 4.05 g/cm^2 carbon reaction target was placed at the F2 dispersive mid-plane. The ^{32}Mg fragments from the one-neutron removal reaction were transported to F4 using the second half of the FRS. Here they were identified using the same principle as above with the TPC, MUSIC and scintillator detectors placed at F4.

To determine the momentum distribution due to one-neutron removal at the target, the FRS was operated in dispersion-matched mode. In this mode, the position distribution at F4 is a measure of the momentum distribution due to the reaction, independent of the initial momentum spread of the ^{33}Mg secondary beam. The energy loss in and the shape of the reaction target at F2 leads to some deviation from this ideal achromatic image condition as observed through a correlation of the horizontal position at the reaction target at F2 and the horizontal position at the F4 focus. This correlation could then be accounted for to improve the achromatic condition by making the position at F4 independent of that at F2.

Reactions occurring in the residual matter (detectors, vacuum windows) were separately measured in a setting where the carbon reaction target was removed. The magnetic rigidity of the second half of FRS was set to transport ^{32}Mg as the central fragment at F4. To subtract these background contributions, the number of ^{32}Mg fragments detected without the carbon target were normalized by the ratio of the incident beam (^{33}Mg) particles measured with and without the target. Fig. 2 shows the normalized background distribution (open circles). This distribution was then subtracted from the distribution with the carbon target (Fig. 2, open squares). The background subtracted momentum distribution is shown in Figs. 3–5. The momentum acceptance of the FRS is shown by the vertical dashed lines in Fig. 2.

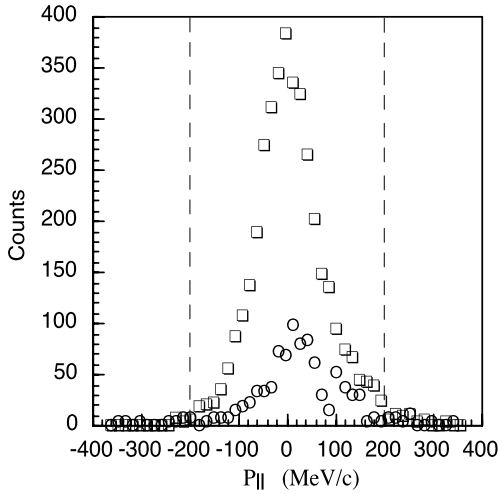

Fig. 2. The longitudinal momentum distribution data for ^{33}Mg $\rightarrow$ ^{32}Mg with carbon reaction target (open squares) and without the carbon reaction target (open circles).

The momentum resolution was determined in a separate setting, where the second half of the FRS was set to transport the unreacted ^{33}Mg beam after the reaction target to F4. The observed momentum distribution fitted by a Gaussian function gives a measure of the resolution as 29.0 ± 0.2 MeV/c (FWHM). The width of the background subtracted distribution for ^{33}Mg $\rightarrow$ ^{32}Mg, shown by the black data points in Fig. 3, was 150 ± 3 MeV/c (FWHM). Accounting for the momentum resolution, the intrinsic width (assuming gaussian shape) is 147 ± 2 MeV/c (FWHM). The one-neutron removal cross-section is 74 ± 4 mb. The error bars shown in Fig. 3 include both statistical and systematic errors. The systematic errors arise from the 1.2% uncertainty in the measured target thickness and the estimated 5% uncertainty in transmission.

The data are interpreted in the framework of eikonal model calculations [30] based on a ^{32}Mg $+ n$ description of ^{33}Mg. The distributions calculated in this model have been folded with the experimental momentum resolution. The wavefunctions for the neutrons were obtained from a Wood–Saxon binding potential, the depth of which was adjusted to reproduce the effective neutron separation energy, including the excitation energy of the ^{32}Mg core for each configuration.

Following the conventional shell model with a shell closure at $N = 20$, the last neutron in ^{33}Mg should occupy the $1f_{7/2}$ orbital. The dotted line in Fig. 3(a) shows the distribution for the $^{32}\mathrm{Mg}_{gs} + n(1f_{7/2})$ configuration with the spectroscopic factor $S = 1$. It can be seen that this configuration does not describe the data either in shape or in magnitude thereby confirming that neutron(s) are distributed differently between the *sd*-shell and the *fp*-shell. This rules out a $7/2^-$ spin assignment in a 0p–0h description of the ground state of ^{33}Mg.

The beta decay studies suggest the ground state of ^{33}Mg to be $3/2^+$ with an odd number of neutron(s) in the $1d_{3/2}$ orbital either in a 1p–1h or a 3p–3h configuration. The solid line in Fig. 3(a) shows the calculated momentum distribution for $^{32}\mathrm{Mg}_{gs} + n(1d_{3/2})$ with a spectroscopic factor of 1.0. This distribution fails as well in reproducing the shape and magnitude of the data.

The relatively narrow width of the momentum distribution suggests neutron removal from orbitals with low angular momentum. We consider neutron removal from the $2p_{3/2}$ orbital, that may be lowered both due to deformation as well as the decreasing neutron separation energy for neutron-rich nuclei. The momentum distribution for the configuration with the ^{32}Mg core in its ground state and one neutron in the $2p_{3/2}$ orbital resulting in a ground state spin of $3/2^-$, is shown by the dashed line in Fig. 3(a) with a

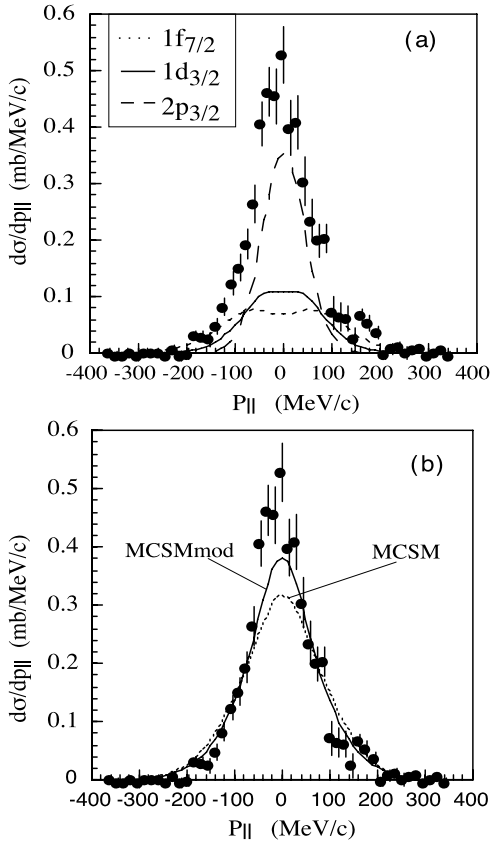

Fig. 3. The longitudinal momentum distribution data for ^{33}Mg $\rightarrow$ ^{32}Mg (filled circles). The curves are eikonal model calculations (a) with the core ^{32}Mg in its ground state coupled to a neutron in the $1f_{7/2}$ orbital (dotted line), $1d_{3/2}$ orbital (solid line) and $2p_{3/2}$ orbital (dashed line), respectively, (b) dashed line (solid line) with the MCSM (MCSMmod) configurations (Table 1). The MCSMmod has the $2p_{3/2}$ orbital lowered by 1 MeV.

spectroscopic factor of unity. Its width of 108 MeV/c (FWHM) is narrower than the data, suggesting that the core ^{32}Mg should also be in an excited state. This would increase the effective separation energy, thereby making the momentum distribution wider.

The Monte Carlo shell model (MCSM) calculation with the SDPF-M interaction, that has been considered to be very successful in describing the island of inversion, predicts the ground state of ^{33}Mg to be $3/2^-$. A highly mixed configuration is predicted with the configurations and spectroscopic factors listed in Table 1. Fig. 3(b). shows that the calculated momentum distribution (dashed line) with the MCSM configurations (Table 1) does not explain the data. The experiment clearly shows the necessity for an enhanced low angular momentum component in the ground state of ^{33}Mg. The modified MCSM calculations with the $2p_{3/2}$ orbital lowered by 1 MeV are shown in Table 1 (MCSMmod) and in Fig. 3(b) by the solid line. This leads to a better reproduction of the momentum distribution. The magnetic moment values predicted by the MCSM is -0.750 while that with the modified MCSM is -0.763 showing that it is minimally affected by the lowering of the $2p_{3/2}$ orbital. Both these values are consistent with the experiment [16]. The present data thus provides a sensitive way to understand the gap between the $1f_{7/2}$ and the $2p_{3/2}$ orbitals which is otherwise not known experimentally yet. The influence of the $2p_{3/2}$ orbital is also discussed to be important towards understanding the magnetic moment of ^{34}Al [31].

We performed a search for a best fit to the data from χ^2 minimization with the spectroscopic factors as free parameters for the following configurations in the $3/2^-$ ground state of ^{33}Mg.

Table 1
Shell model spectroscopic factors for ^{33}Mg → ^{32}Mg using the SDPF-M interaction (MCSM) and modified with lower $2p_{3/2}$ orbital (MCSMmod). J_c is the spin of the ^{32}Mg core state and Energy is its excitation energy. Configurations with $S \geqslant 0.1$ are shown.

J_c	Energy (MeV)	Nl_j	σ_{-n}^{sp} (mb)	$S_{(\mathrm{MCSM})}$	$S_{(\mathrm{MCSMmod})}$	$S(3/2^-)_{fit}$	$S(3/2^+)_{fit}$
0^+	0.00	$2p_{3/2}$	40.12		0.12	$0.6^{+0.3}_{-0.5}$	
0^+	0.00	$1d_{3/2}$	22.39				$0.0^{+0.5}_{-0.0}$
2_1^+	0.89	$2p_{3/2}$	34.13	0.14	0.23	$0.5^{+0.7}_{-0.3}$	
2_1^+	0.89	$1f_{7/2}$	20.87	0.32	0.24	$0.5^{+0.2}_{-0.5}$	
4_1^+	2.32	$1f_{7/2}$	17.93	1.13	0.88		
3^-	2.86	$2p_{3/2}$	24.60				$2.2^{+0.2}_{-0.5}$
3^-	2.86	$1f_{7/2}$	17.23				$1.1^{+0.1}_{-0.5}$
2_2^+	3.01	$2p_{3/2}$	25.82	0.19	0.20		
2_2^+	3.01	$2s_{1/2}$	24.81				$0.1^{+0.0}_{-0.1}$
1_1^-	3.81	$2s_{1/2}$	20.94	0.22	0.21	$0.1^{+0.0}_{-0.1}$	
1_1^-	3.81	$1d_{3/2}$	14.04	0.15	0.14	$1.5^{+1.3}_{-1.3}$	
2_1^-	3.76	$1d_{3/2}$	13.30	0.61	0.57		
2_2^-	3.94	$2s_{1/2}$	20.91	0.29	0.27		
3^-	3.99	$1d_{3/2}$	13.61	0.44	0.39		
3^+	4.00	$2p_{3/2}$	21.96		0.12		
4_2^+	4.39	$1f_{7/2}$	15.94	0.23	0.18		

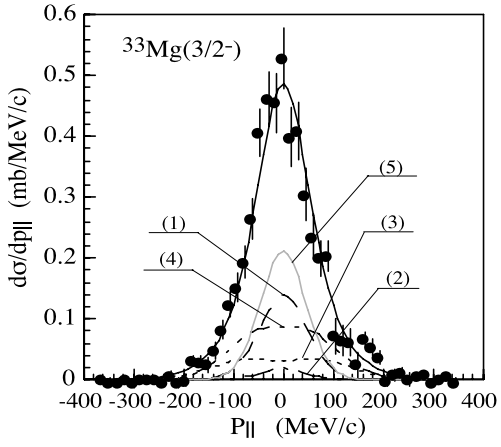

Fig. 4. The longitudinal momentum distribution data for ^{33}Mg → ^{32}Mg (filled circles). The solid line is the eikonal model calculation from the configuration mixing (see text) with a $3/2^-$ ground state for ^{33}Mg. The individual significant configurations obtained from best fit χ^2 search are labeled as (1) $^{32}\mathrm{Mg}_{2_1^+} + \phi_n(2p_{3/2})$, (2) $^{32}\mathrm{Mg}_{1^-} + \phi_n(2s_{1/2})$, (3) $^{32}\mathrm{Mg}_{2_1^+} + \phi_n(1f_{7/2})$, (4) $^{32}\mathrm{Mg}_{1^-} + \phi_n(1d_{3/2})$ and (5) $^{32}\mathrm{Mg}_{gs} + \phi_n(2p_{3/2})$.

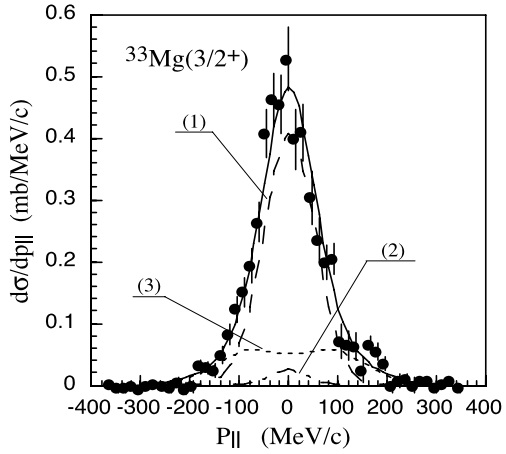

Fig. 5. The longitudinal momentum distribution data for ^{33}Mg → ^{32}Mg (filled circles). The solid line is the eikonal model calculation from the configuration mixing (see text) with a $3/2^+$ ground state for ^{33}Mg. The individual significant configurations obtained from best fit χ^2 search are labeled as (1) $^{32}\mathrm{Mg}_{3^-} + \phi_n(2p_{3/2})$, (2) $^{32}\mathrm{Mg}_{2_2^+} + \phi_n(2s_{1/2})$, (3) $^{32}\mathrm{Mg}_{3^-} + \phi_n(1f_{7/2})$.

The ground state is described by $\alpha_1 \cdot {}^{32}\mathrm{Mg}_{2_1^+}\phi_n(2p_{3/2}) + \alpha_2 \cdot {}^{32}\mathrm{Mg}_{1^-}\phi_n(2s_{1/2}) + \alpha_3 \cdot {}^{32}\mathrm{Mg}_{2_1^+}\phi_n(1f_{7/2}) + \alpha_4 \cdot {}^{32}\mathrm{Mg}_{1^-}\phi_n(1d_{3/2}) + \alpha_5 \cdot {}^{32}\mathrm{Mg}_{gs}\phi_n(2p_{3/2})$. $S_i = \alpha_i^2$ is the spectroscopic factor. The maximum allowed values of the spectroscopic factor are restricted to the respective sum rule values for each case.

The $2s_{1/2}$ orbital in the ^{32}Mg core is occupied in the ground state as well as in the 2^+ excited states. The average occupation number predicted by MCSM is 1.899 and 1.891 for the first two 2^+ states. This would mean that in the configuration for ^{33}Mg there is not much possibility of placing the odd-neutron in the $2s_{1/2}$ orbital outside the ^{32}Mg core. In the configuration mixing considered in the fitting we have therefore restricted the allowed occupancy for the valence neutron of ^{33}Mg to be in the $2s_{1/2}$ orbital to be 0.1.

Fig. 4 shows the best fit (solid) lines to the data with the individual components shown as S_1 (dashed line), S_2 (dashed–dotted line), S_3 (dotted line) and S_4 (dashed–double-dotted line). The resultant spectroscopic factors were found to be $S_1 = 0.5^{+0.7}_{-0.3}$, $S_2 = 0.1^{+0.0}_{-0.1}$, $S_3 = 0.5^{+0.2}_{-0.5}$, $S_4 = 1.5^{+1.3}_{-1.3}$ and $S_5 = 0.6^{+0.3}_{-0.5}$. Inclusion of higher core excited states in the fitting did not lead to any strength in them.

Considering the ground state spin of ^{33}Mg to be $3/2^+$ we looked into a configuration mixing where the ground state can be described by $\alpha_1 \cdot {}^{32}\mathrm{Mg}_{3^-}\phi_n(2p_{3/2}) + \alpha_2 \cdot {}^{32}\mathrm{Mg}_{2_2^+}\phi_n(2s_{1/2}) + \alpha_3 \cdot {}^{32}\mathrm{Mg}_{3^-}\phi_n(1f_{7/2}) + \alpha_4 \cdot {}^{32}\mathrm{Mg}_{gs}\phi_n(1d_{3/2})$. The spectroscopic factors for the different configurations $S_i = (\alpha_i)^2$ were obtained from a χ^2 minimization to the data. The values were found to be $S_1 = 2.2^{+0.2}_{-0.5}$, $S_2 = 0.1^{+0.0}_{-0.1}$, $S_3 = 1.1^{+0.1}_{-0.5}$, $S_4 = 0.0^{+0.5}_{-0.0}$. The resultant momentum distributions are shown in Fig. 5.

Therefore, the important observation in this work is that the narrow observed momentum distribution is a clear signature of significant occupation of the $2p_{3/2}$ orbital. It is much larger than the prediction from the MCSM, which is unable to describe the data. The p-wave spectroscopic strength is larger than that observed for ^{32}Mg from one-neutron removal [27]. In ^{32}Mg the occupancy of the neutron in the $1f_{7/2}$ orbital (1.19(36) [27]) is larger than the $2p_{3/2}$ orbital (0.59(11) [27]). In ^{33}Mg greater oc-

cupancy in $2p_{3/2}$ is observed ($1.1^{+0.76}_{-0.58}$ for $J^{\pi}_{gs} = 3/2^{-}$ and $2.2^{+0.2}_{-0.5}$ for $J^{\pi}_{gs} = 3/2^{+}$) compared to $1f_{7/2}$ ($0.5^{+0.2}_{-0.5}$ for $J^{\pi}_{gs} = 3/2^{-}$ and $1.1^{0.1}_{-0.5}$ for $J^{\pi}_{gs} = 3/2^{+}$). This enhanced probability of neutrons residing in the $2p_{3/2}$ orbital shows the lowering of the $2p_{3/2}$ orbital thereby confirming that the island of inversion is well pronounced beyond $N = 20$. The modified MCSM calculation with the $2p_{3/2}$ orbital lowered by 1 MeV leads to a better reproduction of the data lending support to this view.

Although these nuclei are deformed, in this case we do not employ Nilsson orbitals to interpret the data due to several reasons. It is already known from the study of ^{11,12}Be [24,25] where deformation plays a key role in the inversion of the $2s_{1/2}$ and $1p_{1/2}$ orbitals that the momentum distributions are well explained using spherical single-particle wavefunctions. It was also applied successfully to the study of ^{28}Ne [26] and ^{32}Mg [27]. This reflects the fact that these distributions clearly exhibit the orbital angular momentum of the single-particle orbital. Moreover, the deformation in these neutron-rich nuclei has been understood in the context of particle–hole excitations within the spherical shell model. A Nilsson model that includes orbital re-arrangement in spherical configurations for neutron-rich nuclei is yet to be developed. Furthermore, its extension to reaction theory also needs to be developed. Moreover the excited states of ^{32}Mg do not exhibit the spectrum of a rigid rotor.

In summary, the longitudinal momentum distribution of one-neutron removal from ^{33}Mg was measured at 898A MeV at the FRS of GSI. The one-neutron removal cross-section was measured to be 74 ± 4 mb. The narrow structure of the momentum distribution clearly supports significant occupancy in low angular momentum orbitals. Within the eikonal model, the data could be explained with a large spectroscopic strength for the $2p_{3/2}$ orbital. The data could not be described by the spectroscopic strengths predicted by the MCSM with the SDPF-M interaction. The modified MCSM calculation with the $2p_{3/2}$ orbital lowered by 1 MeV shows an improved agreement with the data. The magnetic moment is found to be less sensitive to this lowering and is consistent with experimental observation both for MCSM and modified MCSM. This shows the lowering of the $2p_{3/2}$ orbital due to deformation and weaker binding in ^{33}Mg. Thus the island of inversion becomes more pronounced across the $N = 20$ gap. The present data has some sensitivity to the relative placing of the $1f_{7/2}$ and $2p_{3/2}$ orbitals which is otherwise not known experimentally yet.

Acknowledgements

The authors are thankful for the support of the GSI accelerator staff and the FRS technical staff for an efficient running of the experiment. The support from NSERC for this work is gratefully acknowledged. R. Kanungo gratefully acknowledges the kind support of the Alexander von Humboldt foundation and the kind hospitality of GSI. This work was supported by the BMBF under contract 06MT238, by the DFG cluster of excellence *Origin and Structure of the Universe*. T. Nilsson is supported by a grant from the Knut and Alice Wallenberg Foundation.

References

[1] B.H. Wildenthal, W. Chung, Phys. Rev. C 22 (1980) 2260.
[2] C. Thibault, et al., Phys. Rev. C 12 (1975) 644.
[3] T. Motobayashi, et al., Phys. Lett. B 346 (1995) 9.
[4] B.V. Pritychenko, et al., Phys. Lett. B 461 (1999) 322.
[5] H. Scheit, et al., Nucl. Phys. A 746 (2004) 96.
[6] K. Yoneda, et al., Phys. Lett. B 499 (2001) 233.
[7] A. Gade, et al., Phys. Rev. Lett. 99 (2007) 072502.
[8] B.V. Pritychenko, et al., Phys. Rev. C 63 (2000) 011305R.
[9] Y. Yanagisawa, et al., Phys. Lett. B 566 (2003) 84.
[10] P. Doornenbal, et al., Phys. Rev. Lett. 103 (2009) 032501.
[11] E.K. Warburton, et al., Phys. Rev. C 41 (1990) 1147.
[12] Y. Utsuno, et al., Phys. Rev. C 60 (1990) 054315.
[13] Y. Utsuno, et al., Phys. Rev. C 64 (2001) 011301R.
[14] T. Otsuka, et al., Phys. Rev. Lett. 87 (2001) 082502.
[15] S. Numella, et al., Phys. Rev. C 64 (2001) 054313.
[16] D.T. Yordanov, et al., Phys. Rev. Lett. 99 (2007) 212501.
[17] V. Tripathi, et al., Phys. Rev. Lett. 101 (2008) 142504.
[18] I. Hamamoto, Phys. Rev. C 76 (2007) 054319.
[19] M. Belleguic, et al., Phys. Rev. C 72 (2005) 054316.
[20] Zs. Dombradi, et al., Phys. Rev. Lett. 96 (2001) 182501.
[21] A. Obertelli, et al., Phys. Lett. B 33 (2006) 633.
[22] V. Tripathi, et al., Phys. Rev. Lett. 94 (2005) 162501.
[23] V. Tripathi, et al., Phys. Rev. C 76 (2007) 021301R.
[24] T. Aumann, et al., Phys. Rev. Lett. 84 (2000) 35.
[25] A. Navin, et al., Phys. Rev. Lett. 85 (2000) 266.
[26] J.R. Terry, et al., Phys. Lett. B 640 (2006) 86.
[27] J.R. Terry, et al., Phys. Rev. C 77 (2008) 014316.
[28] G. Neyens, et al., Phys. Rev. Lett. 94 (2005) 022501.
[29] B.V. Pritychenko, et al., Phys. Rev. C 65 (2002) 061304.
[30] Y. Ogawa, et al., Nucl. Phys. A 571 (1994) 784.
[31] P. Himpe, et al., Phys. Lett. B 658 (2008) 203.